chemistry proceedings

MDPI

Proceeding Paper

Synthesis and *In Silico* Evaluation of Potential Insecticide Activity of Benzamides †

Miguel A. F. Ribeiro [1], Tatiana F. Vieira [2,3], Maria José G. Fernandes [1], Renato B. Pereira [4], David M. Pereira [4], Elisabete M. S. Castanheira [5], A. Gil Fortes [1], Sérgio F. Sousa [2,3] and M. Sameiro T. Gonçalves [1,*]

[1] Centre of Chemistry (CQ/UM), Department of Chemistry, University of Minho, Campus of Gualtar, 4710-057 Braga, Portugal; pg40741@uminho.pt (M.A.F.R.); mjfernandes@quimica.uminho.pt (M.J.G.F.); gilf@quimica.uminho.pt (A.G.F.)
[2] Associate Laboratory i4HB—Institute for Health and Bioeconomy, Faculty of Medicine, University of Porto, 4200-319 Porto, Portugal; tatianafvieira@gmail.com (T.F.V.); sergiofsousa@med.up.pt (S.F.S.)
[3] UCIBIO—Applied Molecular Biosciences Unit, BioSIM—Department of Biomedicine, Faculty of Medicine of University of Porto, Alameda Prof. Hernâni Monteiro, 4200-319 Porto, Portugal
[4] REQUIMTE/LAQV, Laboratory of Pharmacognosy, Department of Chemistry, Faculty of Pharmacy, University of Porto, R. Jorge Viterbo Ferreira, 228, 4050-313 Porto, Portugal; ren.pereira@gmail.com (R.B.P.); dpereira@ff.up.pt (D.M.P.)
[5] Centre of Physics of Minho and Porto Universities (CF-UM-UP), Department of Physics, University of Minho, Campus of Gualtar, 4710-057 Braga, Portugal; ecoutinho@fisica.uminho.pt
* Correspondence: msameiro@quimica.uminho.pt; Tel.: +351-604372
† Presented at the 25th International Electronic Conference on Synthetic Organic Chemistry, 15–30 November 2021; Available online: https://ecsoc-25.sciforum.net/.

Abstract: In order to find alternative pesticides, a series of benzamide derivatives was synthesized. An in silico inverted virtual screening protocol considering the 13 common insecticide protein targets was used to evaluate the potential insecticide activity of these molecules and identify the most likely targets. The results suggest important clues for the development of this class of derivatives as alternative insecticides.

Keywords: benzamides; insecticides; *Spodoptera frugiperda*; pesticides; computational studies

Citation: Ribeiro, M.A.F.; Vieira, T.F.; Fernandes, M.J.G.; Pereira, R.B.; Pereira, D.M.; Castanheira, E.M.S.; Fortes, A.G.; Sousa, S.F.; Gonçalves, M.S.T. Synthesis and in silico evaluation of potential insecticide activity of benzamides. *Chem. Proc.* **2021**, *3*, x. https://doi.org/10.3390/xxxxx

Academic Editor: Julio A. Seijas

Published: 15 November 2021

1. Introduction

Insect resistance to pesticides, resulting from factors like the frequency of resistance alleles, pest management practices and cross-resistance, provoke loss to agriculture and consequences on public health [1–3]. The development of alternative pesticides could help to circumvent this significant limitation.

Carboxamide compounds have shown insecticidal effects against insect pest such as *Spodoptera litura*, or mosquitoes *Aedes aegypti*; the pyrazole carboxamide chlorantraniliprole and the benzamide broflanilide have been placed on the market by agrochemical companies [4–6].

In silico structural-based inverted virtual screening, sometimes mentioned simply as inverted virtual screening or inverse virtual screening, is an appealing methodology to estimate potential protein targets of molecules of pharmacological or biological interest [7,8]. In this methodology, protein-ligand docking is used to predict the binding pose and estimate the binding affinity of a particular molecule of interest towards a database of protein or enzymes of know tridimensional structure, known to be associated with a specific condition or biological effect. Through this methodology, it is possible to identify probable protein targets by screening a protein database with the query ligands, ending up with a subset of the most probable targets for the specific ligands in study.

Considering the above-mentioned facts, and in continuation of our recent interests in pesticides [9–11], in the present work a series of benzamide derivatives was synthesized

in order to predict their potential as insecticides. An in silico inverted virtual screening protocol considering the 13 common insecticide protein targets was used to evaluate the potential insecticide activity of these molecules and identify the most likely targets.

2. Materials and Methods

*2.1. General Procedure for Synthesizing Compounds **4a,b** and **5** (Illustrated for **5**)*

2-Chlorobenzoic acid **1b** (0.372 g, 2.74 mmol) was added to 3-amino-9-ethylcarbazole **3** (0.500 g, 2.74 mmol) and triethylamine (0.995 mL, 7.13 mmol) in dichloromethane. Then, thionyl chloride (0.345 mL, 4.76 mmol) was added at room temperature. The mixture was stirred for 5 days at room temperature, and monitored by TLC (silica: dichloromethane). The recovery of the reaction product was performed by evaporating the solvent under reduced pressure. The resulting residue was taken up in dichloromethane and washed first with 1 M hydrogen chloride (40 mL) and then with 1 M sodium hydroxide (40 mL). The organic phase was dried with magnesium sulfate and evaporated to dryness to afford 2-chloro-N-(9-ethyl-9H-carbazol-3-yl) benzamide **5** as a green solid (0.264 g, 0.856 mmol, 36 %), m.p. = 162–164 °C, R_f = 0.65 (silica: dichloromethane). ^{1}H NMR (400 MHz, $CDCl_3$) δ_H 1.44 (3H, t, J = 7.2 Hz, CH_3), 4.38 (2H, q, J = 7.2 Hz, CH_2), 7.24 (1H, dt, J = 8.0 and 1.2 Hz, H-Ar), 7.39–7.43 (4H, m, Ph-Cl), 7.47–7.51 (2H, m, Ar-H), 7.64 (1H, dd, J = 8.8 and 2.0 Hz, H-Ar), 7.84 (1H, dd, J = 6.8 and 2.4 Hz, Ar-H), 8.06 (1H, s, NH), 8.12 (1H, d, J = 8.0 Hz, Ar-H), 8.47 (1H, d, J = 2.0 Hz, Ar-H) ppm. ^{13}C NMR (100.6 MHz, $CDCl_3$) δ_C 13.79 (CH_3), 37.63 (CH_2), 108.57 (2 × C-PhCl), 113.07 (Ar-C), 118.84 (Ar-C), 119.50 (Ar-C), 120.77 (Ar-C), 122.77 (C-4b), 123.13 (C-4a), 125.95 (Ar-C), 127.29 (Ar-C), 129.31 (PhCl), 130.36 (Ar-C), 130.44 (PhCl), 130.69 (PhCl), 131.52 (PhCl), 135.50 (Ar-C), 137.52 (C-9a), 140.48 (C-8a), 164.68 (C=O) ppm.

2.2. Docking and Inverted Virtual Screening studies

To obtain a representative pool of targets, papers describing virtual screening (VS) studies involving targets and molecules with insecticidal activity were examined throught Scopus. The selection criteria were relevance of the target and year of publication. In the eighteen studies found, thirteen targets were identified and are listed in Table 1.

Table 1. List of targets selected for the Inverted Virtual Screening studies.

	Organism	PDB Target	Resolution (Å)	Ref.
Acetylcholinesterase	*Aedes aegypti*	1QON	2.72	[12]
		4EY6	2.40	
	Drosophila melanogaster	1DX4	2.70	[13]
Alpha-esterase-7 (αE7)	*Lucilia cuprina*	5TYJ	1.75	[14]
		5TYP	1.88	
beta-*N*-Acetyl-D-hexosaminidase OfHex1	*Ostrinia furnacalis*	3NSN	2.10	[15]
		3OZP	2.00	[16]
Chitinase	*Ostrinia furnacalis*	3WL1	1.77	[17]
		3WQV	2.04	
Ecdysone receptor	*Heliothis virescens*	1R20	3	[18]
		1R1K	2.9	[19]
***N*-Acetylglucosamine-1-phosphate uridyltransferase (GlmU)**	*Xanthomonas oryzae*	2V0K	2.3	[20]
		2VD4	1.9	
Octopamine receptor	*Blattella germanica*	4N7C	1.75	[21]
Odorant Binding Protein	*Aedes aegypti*	5V13	1.84	[12]
	Drosophila melanogaster	2GTE	1.4	[22]
	Anopheles gambiae	3N7H	1.6	[23]
	Aedes aegypti	3K1E	1.85	

Peptide deformylase	*Xanthomonas oryzae*	5CY8	2.38	[24]
***p*-Hydroxyphenylpyruvate dioxygenase**	*Arabidopsis thaliana*	6ISD	2.4	[25]
Polyphenol oxidase	*Manduca sexta*	3HSS	2.7	[26]
Sterol carrier protein-2 (HaSCP-2)	*Helicoverpa armigera*	4UEI	Solution NMR	[27]
Voltage-gated sodium channel	*Periplaneta americana*	6A95	2.6	[28]

Each PDB structure was prepared for docking using the Autodock Vina plugin for Pymol [29]. Crystallographic waters were removed. The ligands were extracted and saved in separate files to be used for the re-docking and as reference site for the docking coordinates. When there were no crystallographic ligands present, a selection based on the most important active site residues was made. Re-docking was used to evaluate the ability of the docking software to reproduce the geometry and orientation of the crystallographic pose as well as the quality of the docking protocol, and to optimize the docking protocol.

The docking programs/scoring functions used were GOLD [30] (PLP, ASP, ChemScore,GoldScore), and AutoDock Vina [31]. As a mesasure of protocol quality, redocking was performed. This step is important in the protocol validation stage because it evaluates the predicted docking pose by comparing it to the crystallographic one through a RMSD calculation. The lower the RMSD, the better the docking prediction.

The optimized parameters for each program/scoring function included: center of the docking region, docking box dimension or radius, exhaustivness, search efficiency and number of runs. The final optimized conditions were used for the subsequent stages. The three benzamide derivatives were prepared for docking using Datawarrior [32] and OpenBabel [33] and were docked into each structure with the optimized protocol across the five SF. A ranked list was prepared based on the average scores of each target.

2.3. Molecular Dynamics Simulations and Free Energy Calculations

A 100 ns molecular dynamics simulations were performed using the Amber18 software [34] for the three benzamide derivatives (compounds **4a**, **4b** and **5**) bound to the two most promising targets identified from the inverted virtual screening study (odorant binding protein 1—3KIE and acetylcholinesterase—1QON).

The complexes for the MD simulations were prepared starting from the pose predicted in the inverted virtual screening experiments with GOLD/PLP SF. The molecular mechanics parameters were assigned using ANTECHAMBER, with RESP HF/6-31G(d) charges calculated with Gaussian16 [35] and the General Amber Force Field (GAFF) [36]. The protein targets were described with the ff14SB force field [37]. The protein-ligand complexes were placed in with TIP3P water boxes with a minimum distance of 12 Å between the protein-surface and the side of the box. The overall charge on the system was neutralized through the addition of counter-ions (Na^+) and the periodic boundary conditions were used. Long-range electrostatic interactions were calculated using the particle-mesh Ewald summation method. For short-range electrostatic and Lennard-Jones interactions, a cut-off value of 10.0 Å was used. All bonds involving hydrogen atoms were constrained using the SHAKE algorithm allowing the application of a 2 fs time step.

In order to remove the clashes, the systems were submitted to four consecutive minimizations stages, followed by an equilibration and production. Each minimization had a mazimin of 2500 cycles. After the complete minimization, the systems were equilibrated by a procedure, which was divided into two stages: in the first stage, NVT ensemble, the systems were gradually heated to 298 K using a Langevin thermostat at constant volume (50 ps); in the second stage, the density of the systems was further equilibrated at 298 K (subsequent 50 ps). Finally, the productions runs were performed during 100 ns. Production was executed with an NPT ensemble at constant temperature (298 K, Langevin thermostat) and pressure (1 bar, Berendsen barostat), with periodic boundary conditions. An integration time of 2.0 fs using the SHAKE algorithm was used to constrain all covalent

bonds involving hydrogen atoms. The last 70 ns of the simulation were considered for SASA and hydrogen bonding analysis. This overall procedure has been previously used with success in the treatment of several biomolecular systems 28–35.

The molecular Mechanics/Generalized Born Surface Area method [38] was applied using The MM/PBSA.py [39] script from amber. The last 70 ns of each simulation was analyzed, with an interval of 100 ps and considering a salt concentration of 0.100 mol dm-3. In addition, the energy decomposition method was employed to estimate the contribution of all the amino acid residues for each of these binding free energies. From each MD trajectory, a total of 1400 conformations taken from the last 70 ns of simulation were considered for the MM-GBSA calculations.

3. Results and Discussion

*3.1. Synthesis of Benzamides **4a,b** and **5***

As an attempt to find (semi)synthetic alternative insecticides with high and selective activity to insects, but nontoxic for human cells and environmentally safe, carboxylic amides 4a, 4b and 5 were prepared (Scheme 1). The reaction of 4-chlorobenzoic acid 1a or 2-chlorobenzoic acid 1b and 3-bromoaniline 2, by a known procedure with thionyl chloride and trimethylamine, under room temperature [40], gave *N*-(3-bromophenyl)-4-chlorobenzamide 4a and *N*-(3-bromophenyl)-2-chlorobenzamide 4b. Starting again from 2-chlorobenzoic acid 1b and using 9-ethyl-*9H*-carbazol-3-amine 3, following the same procedure, 2-chloro-*N*-(9-ethyl-*9H*-carbazol-3-yl)benzamide 5 was obtained. All benzamides were isolated in moderate yields and their structures were confirmed by the usual analytical techniques. The ^{1}H NMR of compounds **4a,b** and **5** showed the aromatic protons due to the carboxylic acid units in addition to the amines protons (δ 7.85–8.51 ppm), highlighting the H-3 and H-5 protons of 4-Cl-Ph as double triplets (δ 7.44–7.48 ppm, 4a) and of 2-Cl-Ph as multiplets (δ 7.22–7.47 ppm, 4b, 5), in addition to the H-2 and H-5 protons of 3-Br-Ph as triplets (δ 7.14–7.90 ppm, 4a,b), and of the carbazol nucleus as dublets, double dublets or double triplets (7.22–8.47 ppm, 5). In the ^{13}C NMR stands out the carbon signal of the amide linkage (δ at about 164.5 ppm).

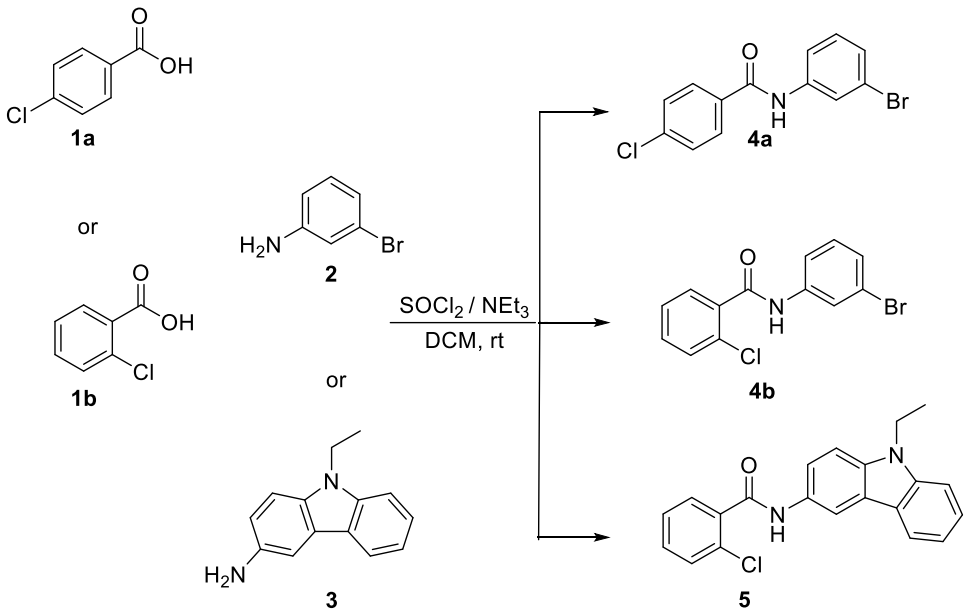

Scheme 1. Synthesis of benzamides **4a**, **4b** and **5**.

3.2. Inverted Virtual Screening results

Table 2 presents the average scores obtained for of all the benzamide derivatives for each potential target with each scoring function. The structure with the best score of each

set of targets was selected and then ranked from the best target to worst, according to the predictions of the different docking programs/scoring functions.

It must be kept in mind that GOLD and Vina SFs are based on different metrics and scales. For the GOLD SFs, the score is dimensionless with a higher value indicatiog a better binding affinity. On the contrary, the Vina scoring function, uses a metric that approximates that of binding free energies and so a more negative value means better affinity.

Table 2. Average scores obtained with the five different scoring functions used and overall ranking.

Target	PDB	PLP	ASP	ChemScore	GoldScore	Vina	Overall Ranking
Acetylcholinesterase	1QON	65.92	43.35	38.89	60.65	−8.37	2
	4EY6	68.27	40.22	38.74	58.03	−9.20	
	1DX4	61.99	39.41	35.60	56.69	−7.60	
alpha-Esterase-7 (αE7)	5TYJ	67.36	37.02	38.75	54.00	−8.23	6
	5TYP	60.73	34.85	35.58	50.38	−7.10	
beta-*N*-Acetyl-D-hexosaminidase OfHex1	3NSN	70.39	40.87	34.48	58.65	−7.67	4
	3OZP	66.80	32.90	33.93	59.54	−8.53	
Chitinase	3WL1	70.75	41.07	35.73	56.36	−8.20	3
	3WQV	70.59	39.42	34.78	57.85	−9.10	
Ecdysone receptor	1R20	63.70	32.55	33.41	52.86	−8.13	5
	1R1K	62.86	31.13	36.74	53.05	−9.07	
***N*-Acetylglucosamine-1-phosphate uridyltransferase (GlmU)**	2V0K	51.73	22.19	25.16	50.72	−7.07	11
	2VD4	46.41	23.58	25.98	41.70	−6.17	
Octopamine receptor	4N7C	42.71	27.27	32.65	31.28	−2.80	12
Odorant Binding Protein	5V13	80.20	47.14	42.51	61.32	−10.53	1
	2GTE	65.24	34.53	38.12	56.36	−7.47	
	3N7H	76.33	40.08	35.80	64.24	−8.30	
	3K1E	85.78	44.69	43.00	66.22	−7.67	
Peptide deformylase	5CY8	69.86	27.06	27.34	59.16	−6.77	8
***p*-Hydroxyphenylpyruvate dioxygenase**	6ISD	59.82	34.04	30.74	50.15	−8.37	9
Polyphenol oxidase	1BUG	46.14	24.86	23.04	48.66	−6.30	13
Sterol carrier protein-2 (HaSCP-2)	4UEI	60.26	32.37	35.79	49.44	−8.77	7
Voltage-gated sodium channel	6A95	55.70	22.09	26.92	50.39	−7.67	10

Overall, the results show good consistency across all the SFs, with odorant binding proteins (OBP), acetylcholinesterases (AChE) and chitinases yielding better scores. Polyphenol oxidase, octopamine receptor and N-acetylglucosamine-1-phosphate uridyltransferase (GlmU), however, are consistently presenting lower scores.

The structures with the best score across all SFs form the OBP (3K1E) and from AChE (1QON) were select selected to move on to MD simulations and Free Energy calculations.

3.3. Molecular Dynamics Simulations and Free Energy Calculations Results

Molecular dynamics simulations were performed for the complexes formed with the benzamide derivatives and the two groups of targets predicted at the inverted VS stage: odorant binding proteins and acetylcholinesterases. The structure with the best score from each group were selected (3K1E for OBP and 1QON for acetylcholinesterases—AChE). The inverted screening predictions were confirmed and further analyzed. Also, the

protein-ligand interactions estabilished were studied and the most determinant residues were defined. The results are present in Table 3.

Table 3. Average RMSD values (Å), ligand RMSF (Å), average SASA (Å²), percentage of potential ligand SASA buried and an average number of hydrogen bonds for the ligands for the last 70 ns of the simulation of the OBP and AChE-ligand complexes.

		Average RMSD of the Complex (Å)	Average RMSD of the Ligand (Å)	Average SASA (Å²)	Percentage of Potential Ligand SASA Buried (%)	Average Number of Hbonds	ΔGbind (kcal/mol)	Main Contributors
OBP	**4a**	2.2 ± 0.2	1.2 ± 0.4	70.8 ± 25.5	83	0.01 ± 0.1	−28.1 ± 0.2	Leu64 (−2.0 ± 0.7); Ala79 (−1.6 ± 0.5); Trp105 (−1.4 ± 1.0)
	4b	2.3 ± 0.4	1.0 ± 0.2	77.4 ± 16.9	82	0.1 ± 0.2	−28.8 ± 0.1	Leu64 (−2.2 ± 0.5); His68 (−1.8 ± 0.5); Ala79 (−1.4 ± 0.3)
	5	2.1 ± 0.2	1.3 ± 0.2	41.9 ± 15.6	93	0.1 ± 0.2	−38.5 ± 0.1	Trp105(−2.4 ± 0.7); Ala79 (−2.3 ± 0.7); Leu67 (−1.8 ± 0.5)
AChE	**4a**	4.6 ± 0.5	0.6 ± 0.3	38.7 ± 19.2	91	0.1 ± 0.3	−25.4 ± 0.1	Tyr69 (−1.5 ± 0.6); Gly148 (−1.3 ± 0.5); Tyr322 (−1.0 ± 0.5)
	4b	2.9 ± 0.2	0.8 ± 0.3	39.9 ± 8.8	91	0.2 ± 0.4	−25.5 ± 0.1	Tyr69 (−2.2 ± 0.6); Tyr368 (−2.0 ± 0.8)
	5	3.0 ± 0.2	0.9 ± 0.2	70.1 ± 21.6	87	0.1 ± 0.3	−32.1 ± 0.2	Tyr372 (−2.8 ± 0.8); Tyr69 (−2.4 ± 0.6); Tyr322 (−1.3 ± 0.7)

When comparing to the initial docking pose, the protein RMSD value for OBP was around 2 Å. For the AChE complexes it was higher, but, the standard deviation was very low. This may indicate that in the beginning of the simulation, the AChE-benzamide complexes were optimized to more stable conformation. The results confirm that all molecules remained bound to their targets and that there is an induced-fit ajustment throughout the simulation.

The solvent accessible surface area (SASA) and the percentage of potential SASA of the ligands that was buried by the target upon binding were also analyzed. A lower SASA accompanied by a high percentage of ligand SASA indicates that the molecule is burried in the target pocket and, therefore, is less exposed to the solvent. For the OBP, it is compound **5** that exhibits the best results, with a SASA of 41.9 Å² and a percentage of burried ligand of 93%. The Gibbs energy of assotiation calculated through, MM/GBSA calculations also indicates that the affinity of compound **5** is stronger toward OBP (−38.5 ± 0.1 versus −32.1 ± 0.2 for AChE). The reverse is true for AChE with compounds **4a** and **4b** presenting a lower SASA (38.7 Å² and 39.9 Å² respectively) and higher percentage of burried ligand (91% for both compounds). However, from all the compounds tested, it is compound **5** that also shows stronger affinity toward AChE (−32.1 kcal/mol vs. −25.4 kcal/mol for compound **4a** and −25.5 kcal/mol for compound **4b**).

When bound to OBP, the compounds are stabilized primarily by electrostatic interactions with Leu64, Ala79 and Trp105. From all the compounds studied, the results seem to suggest that compound **5** can be a good antagonist for OBP. Regarding AChE, the main interacting residues are Tyr69, Tyr322 and Tyr372.

Author Contributions: Conceptualization, M.S.T.G. and S.F.S.; methodology, S.F.S. and M.S.T.G. and; formal analysis, M.S.T.G., M.J.G.F. and S.F.S.; investigation, M.A.F.R. and T.F.V.; writing—original draft preparation, M.S.T.G., M.A.F.R., T.F.V. and S.F.S.; writing—review and editing, M.S.T.G., S.F.S., M.J.G.F., E.M.S.C., D.M.P. and R.B.P.; supervision, M.S.T.G., A.G.F., M.J.G.F. and S.F.S.; project administration, M.S.T.G. All authors have read and agreed to the published version of the manuscript.

Funding: This research was funded by FCT under project PTDC/ASP-AGR/30154/2017 (POCI-01-0145-FEDER-030154) of COMPETE 2020, co-financed by FEDER and EU. FCT-Portugal and FEDER-COMPETE/QREN-EU also gave a financial support to the research centres CQ/UM (UIDB/00686/2020), CF-UM-UP (UIDB/04650/2020) and REQUIMTE (UIDB/50006/2020). The NMR spectrometer Bruker Avance III 400 (part of the National NMR Network) was financed by FCT and FEDER.

Conflicts of Interest: The authors declare no conflict of interest.

References

1. Hawkins, N.J.; Bass, C.; Dixon, A.; Neve, P. The evolutionary origins of pesticide resistance. *Biol. Rev*. **2019**, *94*, 135–155.
2. Curutiu, C.; Lazar, V.; Chifiriuc, M.C. Pesticides and antimicrobial resistance: From environmental compartments to animal and human infections. In *New Pesticides and Soil Sensors*; Grumezescu, A.M., Ed.; Academic Press: 2017, pp. 373–392.
3. The Use of Pesticides in Developing Countries and Their Impact on Health and the Right to Food. Available online: https://www.europarl.europa.eu/thinktank/en/document.html?reference=EXPO_STU%282021%29653622 (accessed on 11 October 2021).
4. Tharamak, S.; Yooboon, T.; Pengsook, A.; Ratwatthananon, A.; Kumrungsee, N.; Bullangpoti, V.; Pluempanupat, W. Synthesis of thymyl esters and their insecticidal activity against Spodoptera litura (*Lepidoptera: Noctuidae*). *Pest Manag. Sci*. **2020**, *76*, 928–935.
5. Deepak, P.; Balamuralikrishnan, B.; Park, S.; Sowmiya, R.; Balasubramani, G.; Aiswarya, D.; Amutha, V.; Perumal, P. Phytochemical profiling of marine red alga, *Halymenia palmata* and its bio-control effects against dengue vector, *Aedes aegypti*. *S. Afr. J. Bot*. **2019**, *121*, 257–266.
6. Jeschke, P. Latest generation of halogen-containing pesticides. *Pest Manag. Sci*. **2017**, *73*, 1053–1066.
7. Huang, H.; Zhang, G.; Zhou, Y.; Chenru, L.; Suling, C.; Yutong, L.; Shangkang, M.; Huang, Z. Reverse screening methods to search for the protein targets of chemopreventive compounds. *Front Chem.* **2018**, *6*, 138.
8. Xu, X., Huang, M., Zou, X. Docking-based inverse virtual screening: Methods, applications, and challenges. *Biophys. Rep.* **2018**, *4*, 1–16.
9. Lopes, A.I.F.; Monteiro, M.; Araújo, A.R.L.; Rodrigues, A.R.O.; Castanheira, E.M.S.; Pereira, D.M.; Olim, P.; Fortes, A.G.; Gonçalves, M.S.T. Cytotoxic plant extracts towards insect cells: Bioactivity and nanoencapsulation studies for application as biopesticides. *Molecules* **2020**, *25*, 5855.
10. Fernandes, M.J.G.; Pereira, R.B.; Pereira, D.M.; Fortes, A.G.; Catanheira, E.M.S.; Gonçalves, M.S.T. New eugenol derivatives with enhanced insecticidal activity. *Int. J. Mol. Sci.* **2020**, *21*, 9257.
11. Natal, C.M.; Fernandes, M.J.G.; Pinto, N.F.S.; Pereira, R.B.; Vieira, T.F.; Rodrigues, A.R.O.; Pereira, D.M.; Sousa, S.F.; Fortes, A.G.; Castanheira, E.M.S.; et al. New carvacrol and thymol derivatives as potential insecticides: Synthesis, biological activity, computational studies and nanoencapsulation. *RSC Adv.* **2021**, *11*, 34024–34035, doi:10.1039/d1ra05616f.
12. Ramos, R.S.; Costa, J.S.; Silva, R.C.; Costa, G.V.; Rodrigues, A.B.L.; Rabelo, E.M.; Souto, R.N.P.; Taft, C.A.; Silva, C.H.T.P.; Rosa, J.M.C.; et al. Identification of potential inhibitors from Pyriproxyfen with insecticidal activity by virtual screening. *Pharmaceuticals* **2019**, *12*, 20.
13. Riva, C.; Suzanne, P.; Charpentier, G.; Dulin, F.; Halm-Lemeille, M.-P.; Santos, J.S.-O. In silico chemical library screening and experimental validation of novel compounds with potential varroacide activities. *Pestic. Biochem. Physiol.* **2019**, *160*, 11–19.
14. 14. Correy, G.J.; Zaidman, D.; Harmelin, A.; Carvalho, S.; Mabbitt, P.D.; Calaora, V.; Peter, J.J.; Kotzeg, A.C.; Jackson, C.J.; London, N. Overcoming insecticide resistance through computational inhibitor design. *Proc. Natl. Acad. Sci. USA* **2019**, *116*, 42, 21012-21021.
15. Liu, J.; Liu, M.; Yao, Y.; Wang, J.; Li, Y.; Li, G.; Yonghua Wang, Y. Identification of novel potential β-*N*-acetyl-D-hexosaminidase inhibitors by virtual screening, molecular dynamics simulation and MM-PBSA calculations. *Int. J. Mol. Sci.* **2012**, *13*, 4545–4563.
16. Dong, L.; Shen, S.; Xu, Y.; Wang, L.; Yang, Q.; Zhang, J.; Lu, H. Identification of novel insect β-*N*-acetylhexosaminidase OfHex1 inhibitors based on virtual screening, biological evaluation, and molecular dynamics simulation. *J. Biomol. Struct. Dyn.* **2021**, *39*, 1735–1743.
17. 17. Dong, Y.; Jiang, X.; Liu, T.; Ling, Y.; Yang, Q.; Zhang, L.; He, X. Structure-based virtual screening, compound synthesis, and bioassay for the design of chitinase inhibitors. *J. Agric. Food Chem.* **2018**, *66*, 3351–3357.
18. Hu, X.; Yin, B.; Cappelle, K.; Swevers, L.; Smagghe, G.; Yang, X.; Zhang, L. Identification of novel agonists and antagonists of the ecdysone receptor by virtual screening. *J. Mol. Graph. Model.* **2018**, *81*, 77–85.
19. Harada, T.; Nakagawa, Y.; Ogura, T.; Yamada, Y.; Ohe, T.; Miyagawa, H. Virtual screening for ligands of the insect molting hormone receptor. *J. Chem. Inf. Model.* **2011**, *51*, 296–305.
20. Min, J.; Lin, D.; Zhang, Q.; Zhang, J.; Yu, Z. Structure-based virtual screening of novel inhibitors of the uridyltransferase activity of *Xanthomonas oryzae* pv. *oryzae* GlmU. *Eur. J. Med. Chem.* **2012**, *53*, 150–158.
21. Offermann, L.R.; Chan, S.L.; Osinski, T.; Tan, Y.W.; Chew, F.T.; Sivaraman, J.; Mok, Y.-K.; Minor, W.; Chruszcz, M. The major cockroach allergen Bla g 4 binds tyramine and octopamine. *Mol. Immunol.* **2014**, *60*, 86–94.
22. Laughlin, J.D.; Ha, T.S.; Jones, D.N.M.; Smith, D.P. Activation of pheromone-sensitive neurons is mediated by conformational activation of pheromone-binding protein. *Cell* **2008**, *133*, 1255–1265.

23. Oliferenko, P.V.; Oliferenko, A.A.; Poda, G.I.; Osolodkin, D.I.; Pillai, G.G.; Bernier, U.R.; Tsikolia, M.; Agramonte, N.M.; Clark, G.G.; Linthicum, K.J.; et al. Promising *aedes aegypti* repellent chemotypes identified through integrated QSAR, virtual ccreening, synthesis, and bioassay. *PLoS ONE* **2013**, *8*, e64547.
24. Joshi, T.; Joshi, T., Sharma, P.; Chandra, S.; Pande, V. Molecular docking and molecular dynamics simulation approach to screen natural compounds for inhibition of *Xanthomonas oryzae pv. Oryzae* by targeting peptide deformylase. *J. Biomol. Struct. Dyn.* **2021**, *39*, 823–840.
25. Fu, Y.; Liu, Y.-X.; Kang, T.; Sun, Y.-N.; Li, J.-Z.; Ye, F. Identification of novel inhibitors of *p*-hydroxyphenylpyruvate dioxygenase using receptor-based virtual screening. *J. Taiwan Inst. Chem. Eng.* **2019**, *103*, 33–43.
26. Fattouch, S.; Raboudi-Fattouch, F.; Ponce, J.V.G.; Forment, J.V.; Lukovic, D.; Marzouki, N.; Vidal, D.R. Concentration dependent effects of commonly used pesticides on activation *versus* inhibition of the quince (*Cydonia Oblonga*) polyphenol oxidase. *Food Chem. Toxicol.* **2010**, *48*, 957–963.
27. Cai, J.; Du, X., Wang, C.; Lin, J.; Du, X. Identification of potential Helicoverpa armigera (*Lepidoptera: Noctuidae*) Sterol Carrier Protein-2 inhibitors through high-throughput virtual screening. *J. Econ. Entomol.* **2017**, *110*, 1779–1784.
28. Shen, H.; Li, Z.; Jiang, Y.; Pan, X.; Wu, J.; Cristofori-Armstrong, B.; Smith, J.J.; Chin, Y.K.Y.; Lei, J.; Zhou, Q.; et al. Structural basis for the modulation of voltage-gated sodium channels by animal toxins. *Science* **2018**, *362*, 1–8.
29. Seeliger, D.; de Groot, B.L. Ligand docking and binding site analysis with PyMOL and Autodock/Vina. *J. Comput. Aided Mol. Des.* **2010**, *24*, 417–422.
30. Jones, G.; Willett, P.; Glen, R.C.; Leach, A.R.; Taylor, R. Development and validation of a genetic algorithm for flexible docking. *J. Mol. Biol.* **1997**, *267*, 727–748.
31. Trott, O.; Olson, A.J. AutoDock Vina: Improving the speed and accuracy of docking with a new scoring function, efficient optimization, and multithreading. *J. Comput. Chem.* **2009**, *31*, 455–461.
32. Sander, T.; Freyss, J.; von Korff, M.; Rufener, C. DataWarrior: An open-source program for chemistry aware data visualization And analysis. *J. Chem. Inf. Model.* **2015**, *55*, 460–473.
33. O'Boyle, N.M.; Banck, M.; James. C.A.; Morley, C.; Vandermeersch, T.; Hutchison, G.R. Open babel: An open chemical toolbox. *J. Cheminform.* **2011**, *3*, 33.
34. Case, D.A.; Cheatham III, T.E.; Darden, T.; Gohlke, H.; Luo, R.; Merz, K.M. Jr.; Onufriev, A.; Simmerling, C.; Wang, B.; Woods, R.J. The Amber biomolecular simulation programs. *J. Comput. Chem.* **2005**, *26*, 1668–1688.
35. Frisch, M.J.; Trucks, G.; Schlegel, H.B.; et al. *Gaussian 09*; Revision A.02; 2016.
36. Wang, J., Wolf, R.M.; Caldwell, J.W.; Kollman, P.A.; Case, D.A. Development and testing of a general amber force field. *J. Comp. Chem.* **2004**, *25*, 1157–1174.
37. Maier, J.A.; Martinez, C.; Kasavajhala, K.;, Wickstrom, L.; Hauser, K.E. Simmerling C. ff14SB: Improving the accuracy of protein side chain and backbone parameters from ff99SB. *J. Chem. Theory Comput.* **2015**, *11*, 3696–3713.
38. Wang, E.; Sun, H.; Wang, J.; Wang, Z.; Liu, H.; Zhang, J.Z.H.; Hou, T. End-point binding free energy calculation with MM/PBSA and MM/GBSA: Strategies and applications in drug design. *Chem. Rev.* **2019**, *119*, 9478–9508.
39. Miller, B.R.; McGee, T.D.; Swails, J.M.; Homeyer, N.; Gohlke, H.; Roitberg, A.E. MMPBSA.py: An efficient program for end-state free energy calculations. *J. Chem. Theory Comput.* **2012**, *8*, 3314–3321.
40. Leggio, A.; Belsito, E.L., De Luca, G., Di Gioia, M.L.; Leotta, V.; Romio, E.; Siciliano, C.; Liguori, A. One-pot synthesis of amides from carboxylic acids activated using thionyl chloride. *RSC Adv.* **2016**, *6*, 34468–34475.